

Nucleation and growth of nickel by electrodeposition under galvanostatic conditions

P. VANDEN BRANDE, A. DUMONT, RENÉ WINAND

Université Libre de Bruxelles, Department Metallurgy-Electrochemistry – CP165, 50, avenue Roosevelt, B1050 Brussels, Belgium

Received 27 January 1993; revised 20 June 1993

The first stages of nickel electrodeposition on amorphous carbon and polycrystalline silver substrates have been studied under galvanostatic conditions. An island growth mode is observed on the two types of substrate. For equivalent conditions the cluster density is higher on silver substrates than on carbon substrates. Dissolution of some nickel clusters is observed a short time after the onset of electrolysis on carbon substrates. This is confirmed by the evolution of the current efficiency and the evolution of the metal surface cluster density as a function of the quantity of electricity.

1. Introduction

Nickel plate is, with or without an underlying copper strike, one of the oldest protective–decorative electrodeposited metallic coatings for steel, brass and other basis metals. On steel sheet, to achieve a good corrosion protection, it is very important to obtain a 100% covering ratio by the nickel layer. A rapid coverage is generally advantageous and can be obtained by the control of the nucleation stage, the growth mode and the coalescence of nickel clusters at the beginning of the deposit formation [1].

The nucleation rate and the cluster critical size of the new-born metallic deposit are functions of the supersaturation, which measures the energetic gap between the out of equilibrium new phase and the equilibrium bulk metallic phase. In electrodeposition the supersaturation, ΔG , is a function of the cathodic overvoltage η [2, 3]:

$$\Delta G = ze\eta$$

where z is the number of exchanged electrons and e is the electron charge.

The cluster critical size, which corresponds to the maximum cluster free energy or to the size for which the probability of cluster growth is higher than the cluster decay probability for a given supersaturation, is proportional to $\sigma^3/\Delta G^3$, where σ is the cluster mean surface specific energy. When the supersaturation increases, the cluster critical size decreases and, in practice, is less than a few atoms [4, 5]. Information on the nuclei comes generally from the interpretation of the cluster density distribution as a function of time (or the quantity of deposited matter) through a nucleation model. In practice, this model is necessarily atomistic and not capillary because for very small clusters, thermodynamic properties (e.g. the specific surface energy and the free energy) lose their physical sense [4–7].

The growth mode depends mainly on the

deposit-substrate interaction, relative to the deposit cohesion. Let E_a denote the deposit atomic adsorption energy and E_c the deposit atomic cohesion energy. Two very different situations are possible: the first, (when $E_a < E_c$) induces an island growth mode (Volmer–Weber), although the second (for which $E_a > E_c$) corresponds to a layer-by-layer growth process (Frank–van der Merwe) [8].

The aim of this paper is to study the first stages of the formation of a nickel electrodeposit against the deposition rate in two situations: the first when $E_a < E_c$ and the second when $E_a > E_c$. The first situation should be obtained on an amorphous carbon substrate because of the probably weak bonding energy between amorphous carbon and electrodeposited nickel. This was indirectly shown by Amblard [9] who transferred electrodeposited nickel clusters grown on a glossy carbon substrate to a thin carbon film for observation in transmission electron microscope (TEM). In contrast, on a polycrystalline silver substrate, the bond between the substrate material and the deposit material is metallic and E_a must be in the same range as E_c , so that the second situation should be obtained.

2. Experimental methods

2.1. Nickel electrodeposition conditions

Nickel was electrodeposited under galvanostatic conditions. These conditions were achieved in a flow through channel cell which allowed good reproducibility for the hydrodynamic conditions. The flow velocity was 2.2 ms^{-1} in approaching the cathode. The electrolyte was a 70 g dm^{-3} -NiSO₄, 30 g dm^{-3} -H₃BO₃ solution deaerated by nitrogen flow. Sulphuric acid was added to the solution in order to regulate the pH between 1.2 and 1.3. The electrolyte temperature was regulated at 323 K.

To be able to use transmission electron microscopy

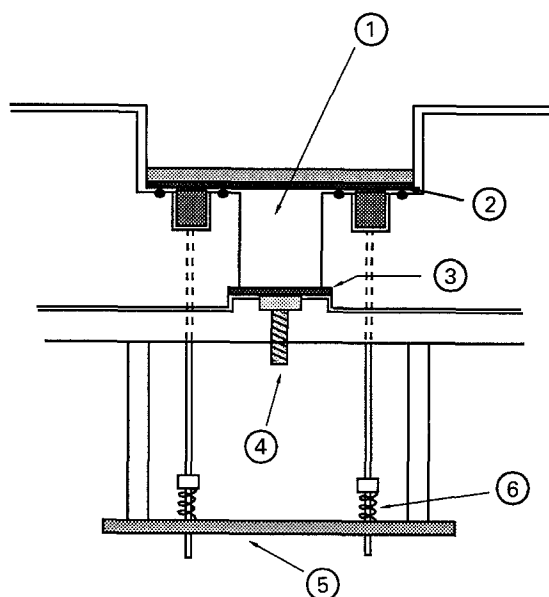


Fig. 1. Cross-section of the electrodeposition cell for thin film substrates. (1) Electrolyte channel; (2) thin conducting film (cathode); (3) anode; (4) anode current lead; (5) cathode current lead; (6) spring.

(TEM) to study small metal crystallites, a deposition technique on thin film substrates of a layered type was developed (Fig. 1). The first layer was a silver conducting layer of about 50 nm. If the substrate surface was made of amorphous carbon, a 10 nm carbon layer was laid on the silver layer. The mechanical support of the thin film substrate was a glass plate. The thickness of the film substrate was large enough to be equipotential under the chosen experimental conditions and small enough to be transparent to the electrons in TEM.

2.2. Production of substrates

The different layers constituting the substrate were deposited by vacuum vapour deposition on a glass plate; the carbon vapour was produced in a d.c. electric arc discharge while the silver vapour was obtained by heating silver in a molybdenum crucible. With calibrated experimental procedures, good reproducibility of the substrate surface was achieved.

2.3. Analytical techniques

The deposits were directly observed by TEM. Pictures of the deposits were digitized for computer analysis by a specially developed program [3]. In this way, information was obtained on the cluster size evolution, cluster surface density and covering ratio. These results were compared with the chemically measured nickel deposited quantities (by atomic absorption after dissolution of the deposit in nitric acid). These last results also allowed the determination of the current efficiency.

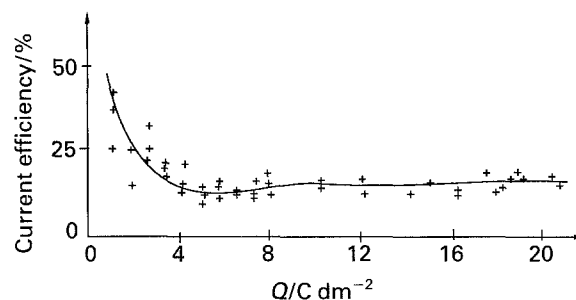


Fig. 2. Current efficiency against quantity of electricity, Q , for nickel electrodeposited on an amorphous carbon substrate ($J = 0.2 \text{ A dm}^{-2}$).

3. Experimental results

3.1. Nickel electrodeposits on amorphous carbon substrates

An island growth mode was observed for two current densities: 0.2 A dm^{-2} and 8 A dm^{-2} .

3.1.1. Current efficiency. At constant current density, the current efficiency always decreases at the beginning of electrolysis (Figs 2 and 3) between approximately 1 C dm^{-2} and 10 C dm^{-2} . It is important to note that the measure of the current efficiency in the very early stages of the film formation (before 1 C dm^{-2}) was not possible. This decrease was from 50% to 25% for $J = 8 \text{ A dm}^{-2}$. For $J = 0.2 \text{ A dm}^{-2}$ the current efficiency decreases down to 15%. After this minimum the current efficiency stays constant ($J = 0.2 \text{ A dm}^{-2}$) or increases against the quantity of electricity (Q) for $J = 8 \text{ A dm}^{-2}$. For higher Q values it seems that, globally, the current efficiency increases with current density (Figs 2 and 3).

3.1.2. Superficial density of clusters as a function of time. At constant current density, J , the cluster surface density, N , decreases when the quantity of electricity Q increases (Fig. 4). The cluster superficial density is in the same range (10^{14} m^{-2}) for the two current densities, while the cluster density is always higher for $J = 0.2 \text{ A dm}^{-2}$ than for $J = 8 \text{ A dm}^{-2}$ at a given Q .

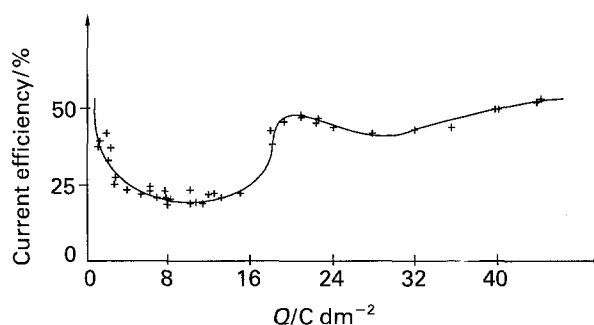


Fig. 3. Current efficiency against quantity of electricity, Q , for nickel electrodeposited on an amorphous carbon substrate ($J = 8 \text{ A dm}^{-2}$).

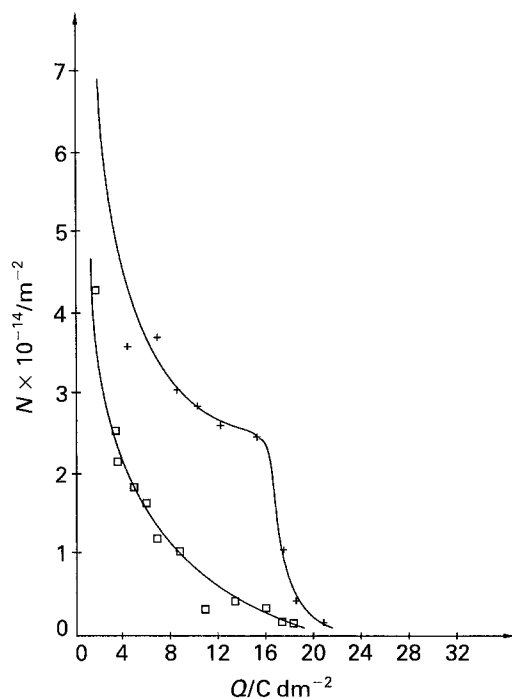


Fig. 4. Cluster superficial density, N , against quantity of electricity, Q , for nickel electrodeposited on an amorphous carbon substrate. (+) $J = 0.2 A dm^{-2}$, (□) $J = 8 A dm^{-2}$.

3.1.3. Evolution of cluster mean size and covering ratio.

The mean apparent surface of clusters, S , is a growing function of Q at constant current density, J , with S always higher at $8 A dm^{-2}$ than at $0.2 A dm^{-2}$ (Fig. 5). The covering ratio, T_c , also increases against Q (Fig. 6). However, due to the lower cluster density observed at $8 A dm^{-2}$, T_c is only slightly higher at $8 A dm^{-2}$ than at $0.2 A dm^{-2}$ (Fig. 6).

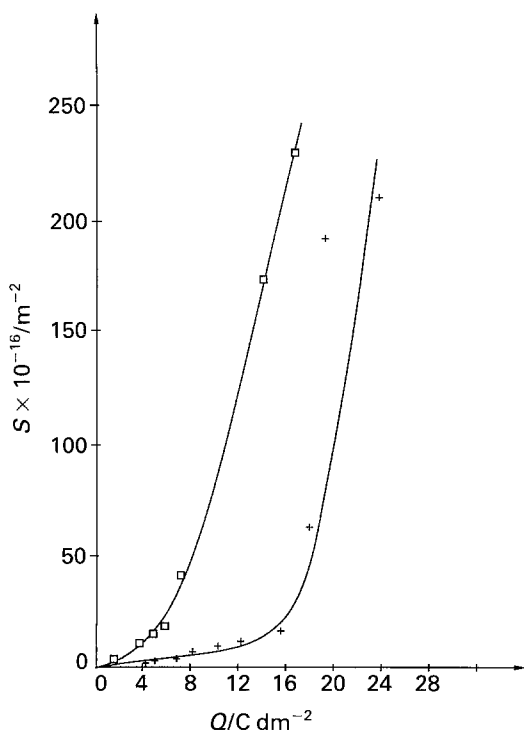


Fig. 5. Cluster mean apparent surface, S , against quantity of electricity, Q , for nickel electrodeposited on an amorphous carbon substrate (+) $J = 0.2 A dm^{-2}$, (□) $J = 8 A dm^{-2}$.

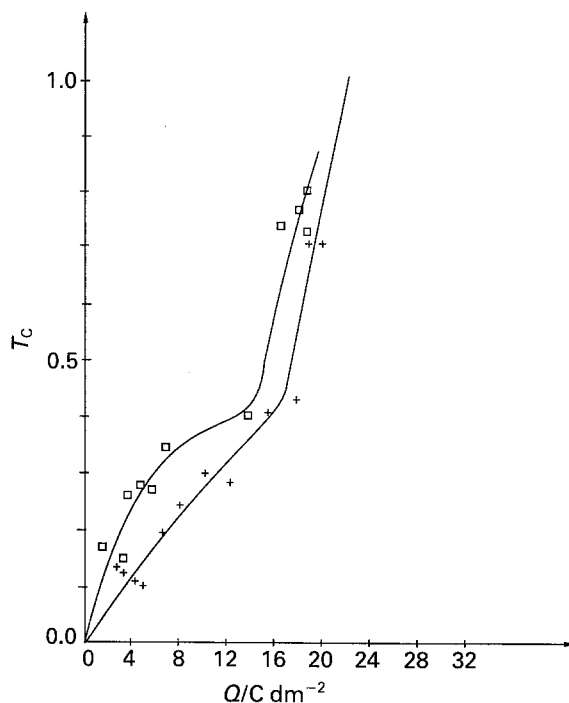


Fig. 6. Covering ratio, T_c , against quantity of electricity, Q , for nickel electrodeposited on an amorphous carbon substrate. (+) $J = 0.2 A dm^{-2}$, (□) $J = 8 A dm^{-2}$.

3.2. Nickel electrodeposits on polycrystalline silver substrates

Nickel electrodeposits were produced at $2 A dm^{-2}$ on silver substrates. No cluster was observed by TEM on the silver thin film substrates and the use of an Auger method was necessary to characterize the deposits.

3.2.1. Current efficiency. The current efficiency (c.e.) is presented against Q for nickel electrodeposited on silver polycrystalline substrates at a current density $J = 2 A dm^{-2}$. The current efficiency increases with Q (Fig. 7).

3.2.2. Auger electron spectroscopy. Auger electron spectroscopy (AES) was performed to determine the growth mode of the nickel deposit on the silver substrate. The nickel-to-silver peak-to-peak Auger signal against the quantity of deposited matter expressed in $C dm^{-2}$ ($Q \times c.e.$) or by the number, e , of equivalent deposited nickel atomic layers (Fig. 8) has a characteristic evolution depending on

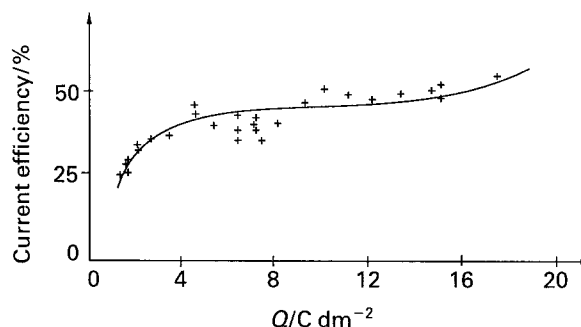


Fig. 7. Current efficiency against quantity of electricity, Q , for nickel electrodeposited on a polycrystalline silver substrate. ($J = 2 A dm^{-2}$).

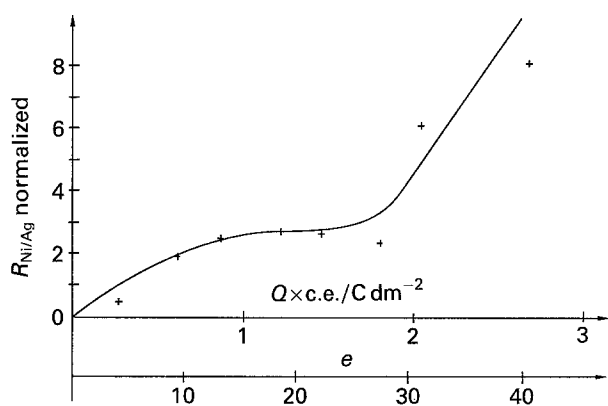
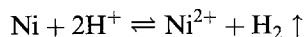


Fig. 8. Experimental deposit-to-substrate Auger peak-to-peak intensity ratio, R , as a function of $Q \times \text{c.e.}$ or the equivalent deposited atomic layers number e of nickel electrodeposited on a silver substrate for $J = 2 \text{ A dm}^{-2}$.

the growth mode [10]. This curve presents a characteristic plateau between $Q \times \text{c.e.} = 0.8 \text{ C dm}^{-2}$ and $Q \times \text{c.e.} = 1.8 \text{ C dm}^{-2}$. More detail of the analysis method and the derivation of the curve in Fig. 8, may be found in [10].

4. Discussion

On carbon substrates the decrease in current efficiency (c.e.) observed at constant current density at the beginning of the electrolysis ($> 1 \text{ C dm}^{-2}$) is related to the decrease in nickel cluster surface density. This means that dissolution of some nickel clusters occurs at the beginning of the electrodeposition process, probably via the reaction



Subsequently the current efficiency is constant and equal to 15% for $J = 0.2 \text{ A dm}^{-2}$ or increases against Q when $Q > 16 \text{ C dm}^{-2}$ for $J = 8 \text{ A dm}^{-2}$ (Figs 2 and 3). This increase probably corresponds to the end of the cluster dissolution with island growth and coalescence (Figs 5 and 6) as will be explained in more detail in the following paragraph. Nickel dissolution may be tentatively explained as follows. When an island grows, the current flow lines and the pattern of equipotentials in the electrolyte change. This induces a decrease in the current density and also a decrease in the overvoltage around the island. A small cluster, supercritical where no large island is growing, can become undercritical in the vicinity of such a large growing island. This undercritical cluster dissolves in the electrolyte resulting in so-called exclusion zones [3]. This explains, as seen above, the decrease of c.e. against Q in the early stages of the electrolysis. When small clusters are in the exclusion zones of big islands the current efficiency decreases up to the time where all these clusters are dissolved. At this moment the current efficiency remains constant or increases.

Coalescence of the clusters is characterized by the increase in the slope of the curves in Fig. 6 at Q values higher than 16 C dm^{-2} and by the high values of the cluster mean apparent surface (Fig. 5). When the

covering ratio T_c reaches 100%, the current efficiency c.e. is under 100%. The highest measured current efficiency is 15% for $J = 0.2 \text{ A dm}^{-2}$ and 50% for $J = 8 \text{ A dm}^{-2}$. This phenomenon is well known in nickel electrodeposition: the low hydrogen overvoltage on the nickel surface results in hydrogen evolution. When the current density increases the current efficiency increases because that part of the current density used for nickel electrodeposition increases in comparison to the hydrogen evolution current density.

The nickel cluster surface density decreases and the cluster mean apparent surface area increases with current density. This phenomenon cannot be attributed to nucleation because a higher value of the current density corresponds to a higher supersaturation and, accordingly, to a higher nucleation rate [3, 8]. A tentative explanation could be that the cluster surface density and the cluster mean area are controlled by a passivation mechanism of the substrate surface which dominates the nucleation process. In that case, any current density increase would result in an increase in the passivated substrate area, thus decreasing the nickel cluster density. This passivation layer could be an hydroxide because protons are consumed near the cathode. In some parts of the cathode the solution was shown to reach a pH equal to or higher than 6 so that nickel hydroxide may be locally precipitated [11].

The significant nickel loss observed on carbon substrates and characterized by significant decrease in current efficiency at the beginning of electrodeposition is not observed on silver substrates. In this case the current efficiency is only a growing function of Q . Following [10], the evolution of the nickel-to-silver peak-to-peak intensity ratio, R , as a function of the quantity of deposited nickel ($Q \times \text{c.e.}$ or e), should be characteristic of an island growth mode followed by a coalescence stage because of the presence of a plateau followed by a rapid increase in R (Fig. 8). The mean apparent surface of a cluster and the mean cluster surface density have been estimated from this curve, assuming an identical volume per cluster equal to the mean cluster volume of the real distribution and assuming a given geometry for the clusters. For a cubic geometry the area, S , of the cluster apparent surface was found to be 34.65 nm^2 and the cluster mean surface density to be $2.88 \times 10^{16} \text{ m}^{-2}$ [10]. This cluster mean surface density is two orders of magnitude higher than the cluster surface density found on carbon substrates. This probably explains why clusters were not observed by TEM on silver substrates. The higher cluster surface density on silver substrates than on carbon substrates is probably due to the higher adhesion energy between nickel and silver than between nickel and amorphous carbon because when the adhesion energy increases, for a given supersaturation, the nucleation rate increases [3, 8].

5. Conclusion

In this paper we have shown that the first stages of nickel electrodeposition display an apparent island growth mode on amorphous carbon substrates as well as on silver. On amorphous carbon substrates a Volmer–Weber growth mode is observed because $E_a < E_c$.

The evolution of the current efficiency with Q and the TEM observation of the nickel deposits on carbon substrates before the coalescence stage, at a constant current density J , show that nickel clusters dissolve in the early stages of electrolysis. The dissolving clusters are probably those which enter the exclusion zones of growing islands.

The decrease in cluster surface density and the increase in cluster mean apparent area on carbon substrates with increase in current density may be explained in terms of the passivation of the substrate surface by a nickel hydroxide precipitate which dominates the nucleation process.

Thus the passivation process seems to be the critical factor rather than the nucleation stage in achieving rapid coalescence of the deposit.

Acknowledgements

The authors thank Le Centre de Recherches et Développements du Groupe Cockerill–Sambre (RDSC) as well as La Région Wallonne and the National Fund for the Scientific Research (FNRS), two Belgian Governmental organizations, for partial financial support.

References

- [1] P. Vanden Brande, Thesis, Université Libre de Bruxelles, Service Métallurgie-Electrochimie, Bruxelles (1985).
- [2] K. J. Vetter, 'Elektrochemische Kinetik', Springer Verlag, Berlin (1961).
- [3] P. Vanden Brande, Ph.D. Thesis, Université Libre de Bruxelles, Service Métallurgie-Electrochimie, Bruxelles (1990).
- [4] A. Milchev, *Electrochim. Acta* **28** (1983) 947.
- [5] A. Milchev and S. Stoyanov, *J. Electroanal. Chem.* **72** (1976) 33.
- [6] *Idem*, *Thin Solid Films* **22** (1974) 255.
- [7] *Idem*, *ibid.* **22** (1974) 267.
- [8] B. Lewis and J. C. Anderson, 'Nucleation and Growth of Thin Films', Academic Press, NY (1978).
- [9] J. Amblard, M. Froment, G. Maurin, N. Spyrellis and E. Trevisan-Southeyrand, *Electrochim. Acta* **28** (1983) 909.
- [10] P. Vanden Brande and R. Winand, *Thin Solid Films* **220** (1992) 204.
- [11] S. Baudhuin, Thesis, Université Libre de Bruxelles, Service Métallurgie-Electrochimie, Bruxelles (1984).